

# 1 Geoeffectiveness and efficiency of CIR, sheath, 2 and ICME in generation of magnetic storms

3 Y. I. Yermolaev,<sup>1</sup> N. S. Nikolaeva,<sup>1</sup> I. G. Lodkina,<sup>1</sup> and M. Y. Yermolaev<sup>1</sup>

4 Received 5 September 2011; revised 25 March 2012; accepted 28 March 2012; published XX Month 2012.

5 [1] We investigate the relative role of various types of solar wind streams in generation of  
6 magnetic storms. On the basis of the OMNI data of interplanetary measurements for the  
7 period of 1976–2000, we analyze 798 geomagnetic storms with  $Dst \leq -50$  nT and five  
8 various types of solar wind streams as their interplanetary sources: corotating interaction  
9 regions (CIR), interplanetary coronal mass ejection (ICME) including magnetic clouds  
10 (MC) and ejecta, and a compression region sheath before both types of ICME ( $SHE_{MC}$   
11 and  $SHE_{Ej}$ , respectively). For various types of the solar wind we study the following  
12 relative characteristics: occurrence rate; mass, momentum, energy and magnetic fluxes;  
13 probability of generation of a magnetic storm (geoeffectiveness); efficiency of the  
14 process of this generation; and solar cycle variation of some of these parameters.  
15 Obtained results show that in spite of the fact that magnetic clouds have lower  
16 occurrence rates and lower efficiency than CIR and sheath, they play an essential role in  
17 generation of magnetic storms due to higher geoeffectiveness of storm generation (i.e.,  
18 higher probability to contain large and long-term southward IMF  $B_z$  component).  
19 Geoeffectiveness for all drives is at the smallest during a solar cycle minimum and  
20 increases at other phases of the cycle.

21 **Citation:** Yermolaev, Y. I., N. S. Nikolaeva, I. G. Lodkina, and M. Y. Yermolaev (2012), Geoeffectiveness and efficiency of  
22 CIR, sheath, and ICME in generation of magnetic storms, *J. Geophys. Res.*, 117, AXXXXX, doi:10.1029/2011JA017139.

## 23 1. Introduction

24 [2] One of the key issues of solar-terrestrial physics is  
25 investigation of mechanisms of energy transfer from the solar  
26 wind into the magnetosphere and of excitation of magneto-  
27 spheric disturbances. As has been discovered by direct space  
28 experiments in the beginning of 1970s, the basic parameter  
29 leading to magnetospheric disturbances is negative (south-  
30 ward)  $B_z$  component of the interplanetary magnetic field  
31 (IMF) (or electric field  $E_y = Vx \times B_z$ ) [Dungey, 1961;  
32 Fairfield and Cahill, 1966; Rostoker and Falthammar, 1967;  
33 Russell et al., 1974; Burton et al., 1975; Akasofu, 1981].  
34 [3] Numerous investigations demonstrated that IMF in the  
35 undisturbed solar wind lies in the ecliptic plane (i.e.,  $B_z$  is  
36 close to zero) and only disturbed types of the solar wind  
37 streams can have a considerable value of IMF  $B_z$ . The  
38 interplanetary coronal mass ejection (ICME) with a com-  
39 pression region sheath before it and the compression region  
40 between slow and fast solar wind streams (corotating inter-  
41 action region (CIR)) belong to such types of solar wind  
42 streams (see reviews and recent papers, for instance, by  
43 Tsurutani et al. [1988], Tsurutani and Gonzalez [1997],

Gonzalez et al. [1999], Yermolaev and Yermolaev [2002], 44  
Huttunen and Koskinen [2004], Echer and Gonzalez [2004], 45  
Yermolaev and Yermolaev [2006], Borovsky and Denton 46  
[2006], Denton et al. [2006], Huttunen et al. [2006], 47  
Yermolaev et al. [2007a, 2007b, 2007c], Pulkkinen et al. 48  
[2007a, 2007b], Zhang et al. [2007], Turner et al. [2009], 49  
Xu et al. [2009], Yermolaev et al. [2010a, 2010b, 2010c, 50  
2010d, 2011], Nikolaeva et al. [2011, 2012], Alves et al. 51  
[2011], Echer et al. [2011], Gonzalez et al. [2011], Guo 52  
et al. [2011], Mustajab and Badruddin [2011], and refer- 53  
ences therein). 54

[4] Experimental results have shown that the magneto- 55  
spheric activity induced by different types of interplanetary 56  
streams is different [Borovsky and Denton, 2006; Denton 57  
et al., 2006; Huttunen et al., 2006; Pulkkinen et al., 2007a; 58  
Plotnikov and Barkova, 2007; Longden et al., 2008; Turner 59  
et al., 2009; Despirak et al., 2009, 2011; Guo et al., 2011]. 60

[5] This fact indicates that it is necessary to take into 61  
account the influence of other (in addition to IMF  $B_z$  and 62  
electric field  $E_y$ ) parameters of the solar wind, dynamics of 63  
parameter variation, and different mechanisms of generating 64  
the magnetospheric disturbances at different types of the 65  
solar wind streams. Several recent papers analyzed separ- 66  
ately CIR, sheath and body of ICME and compared them 67  
with each other [Huttunen and Koskinen, 2004; Yermolaev 68  
and Yermolaev, 2006; Huttunen et al., 2006; Yermolaev 69  
et al., 2007a, 2007b, 2007c; Pulkkinen et al., 2007a; 70  
Yermolaev and Yermolaev, 2010; Yermolaev et al., 2010a, 71  
2010b, 2011; Alves et al., 2011; Despirak et al., 2011; 72  
Nikolaeva et al., 2011, 2012; Guo et al., 2011]. 73

<sup>1</sup>Space Plasma Physics Department, Space Research Institute, Russian Academy of Sciences, Moscow, Russia.

Corresponding Author: Y. I. Yermolaev, Space Plasma Physics Department, Space Research Institute, Russian Academy of Sciences, Prof. 84/32, Moscow 117997, Russia. (yermol@iki.rssi.ru)

Copyright 2012 by the American Geophysical Union.  
0148-0227/12/2011JA017139

74 [6] The papers mentioned above are devoted to studying a  
 75 response of the magnetosphere to interplanetary drives, and  
 76 they use the word *geoeffectiveness* to designate this link. It  
 77 should be noted that in the literature the *geoeffectiveness* is a  
 78 double meaning term [see *Yermolaev and Yermolaev*, 2006,  
 79 2010]. In one case, *geoeffectiveness* implies a probability  
 80 with which a selected phenomenon can cause a magnetic  
 81 storm, i.e., the ratio between the number of events  $K^j$  of a  
 82 chosen stream type  $j$  (MC, CIR etc.) resulting in a magnetic  
 83 storm with  $Dst < Dst_0$  and the total number of this type  
 84 events  $N^j$ :  $P^j = K^j/N^j$ . In the other case, *geoeffectiveness*  
 85 implies the efficiency of storm generation by unambiguously  
 86 interrelated phenomena, i.e., the ratio between the “output”  
 87 and “input” of a physical process, for example, between the  
 88 values of the  $Dst$  index and the southward IMF  $Bz$  compo-  
 89 nent. To avoid ambiguity of the term *geoeffectiveness* we  
 90 will use below the term *geoeffectiveness* for a designation of  
 91 probability of relation between the phenomena and the term  
 92 *efficiency* for a designation of efficiency of process relating  
 93 phenomena.

94 [7] Magnetospheric activity induced by different inter-  
 95 planetary drivers depends on the following parameters: (1)  
 96 occurrence rate of these drivers near the Earth, (2) occur-  
 97 rence rate of corresponding geoeffective conditions in these  
 98 drivers, and (3) ability (efficiency) of these conditions in  
 99 various drivers to induce magnetospheric disturbances. Only  
 100 several of these parameters for separate types of storm dri-  
 101 vers have been estimated in the literature.

102 [8] The occurrence rate of magnetic clouds (MC) is ana-  
 103 lyzed in a great number of works, but only in several papers  
 104 their authors compare occurrence rates of several types of  
 105 the solar wind streams. For instance, occurrence rates of MC  
 106 and ejecta are compared by *Cane and Richardson* [2003],  
 107 *Richardson and Cane* [2004], and *Lepping and Wu* [2010];  
 108 occurrence rates of MC and  $SHE_{MC}$  by *Huttunen et al.*  
 109 [2005]; and occurrence rates of CIR, ejecta and  $SHE_{Ej}$  by  
 110 *Dmitriev et al.* [2005] and *Jian et al.* [2008]. In the present  
 111 work we simultaneously consider the occurrence rates of  
 112 5 interplanetary drivers: CIR, MC, ejecta,  $SHE_{MC}$  and  $SHE_{Ej}$   
 113 (as well as combinations of them ICME = MC + ejecta and  
 114 sheath =  $SHE_{MC} + SHE_{Ej}$ ) during 1976–2000.

115 [9] Numerous papers are devoted to investigations of  
 116 *geoeffectiveness* in generation of magnetic storm. Many  
 117 works study *geoeffectiveness* of magnetic clouds, while  
 118 *geoeffectiveness* of other phenomena is studied rather poorly  
 119 (see, for example, recent reviews and papers by *Yermolaev*  
 120 *and Yermolaev* [2006, 2010] and *Alves et al.* [2011]). So,  
 121 one of the main aims of this paper is to investigate *geof-*  
 122 *fectiveness* of various interplanetary drivers and to compare  
 123 them to each other.

124 [10] Efficiencies of various interplanetary drivers vary  
 125 with the type of solar wind streams and may be estimated as  
 126 the ratio of measured energy output to estimated energy  
 127 input (see, for example, papers by *Turner et al.* [2009],  
 128 *Yermolaev et al.* [2010c], and references therein). In our  
 129 previous and present investigations we use  $Bz$  ( $E_y$ ) and  
 130 magnetospheric indices  $Dst$ ,  $Dst^*$  (pressure corrected  $Dst$ ),  
 131  $Kp$  and  $AE$  as “input” and “output” of the storm generation  
 132 processes for the estimation of efficiency of interplanetary  
 133 drivers.

134 [11] In the present work we simultaneously consider for  
 135 the first time the entire set of these parameters (occurrence

rate (section 3.1), *geoeffectiveness* (section 3.2) and effi- 136  
 ciency (section 3.3.)) for the magnetic storms generated by 137  
 5 types of interplanetary drivers (CIR, MC, ejecta,  $SHE_{MC}$  138  
 and  $SHE_{Ej}$ ). In addition, in the present work we include 139  
 (1) comparative characteristics of mass, momentum, energy 140  
 and magnetic field fluxes for various drivers (section 3.1); 141  
 (2) numerical estimations of efficiency of various geomag- 142  
 netic activity for various drivers (section 3.3); and (3) solar 143  
 cycle variation of parameters. 144

## 2. Methods 145

[12] When the types of solar wind streams were classified, 146  
 we used the OMNI database (see [http://omniweb.gsfc.nasa.](http://omniweb.gsfc.nasa.gov) 147  
[gov](http://omniweb.gsfc.nasa.gov) [*King and Papitashvili*, 2005]) for interval 1976–2000, 148  
 available world experience in identification of solar wind 149  
 streams and the standard criteria for the following para- 150  
 meters: velocity  $V$ , density  $n$ , proton temperature  $T$ , ratio of 151  
 thermal to magnetic pressure ( $\beta$  parameter), ratio of mea- 152  
 sured temperature to temperature calculated on the basis of 153  
 average “velocity–temperature” relation  $T/T_{exp}$  [*Lopez*, 154  
 1987], thermal pressure and magnetic field. This method 155  
 allows us to identify reliably 3 types of quasi-stationary 156  
 streams of the solar wind (heliospheric current sheet (HCS), 157  
 fast streams from the coronal holes, and slow streams from 158  
 the coronal streamers), and 5 disturbed types (compression 159  
 regions before fast streams (CIR), and interplanetary mani- 160  
 festations of coronal mass ejections (ICME) that can include 161  
 magnetic clouds (MC) and ejecta with the compression 162  
 region sheath ( $SHE_{MC}$  and  $SHE_{Ej}$ ) preceding them). In 163  
 contrast with ejecta, MCs have lower temperature, lower 164  
 ratio of thermal to magnetic pressure ( $\beta$  parameter) and 165  
 higher, smooth and rotating magnetic field [*Burlaga*, 1991]. 166  
 In addition, we have included into our catalog direct and 167  
 reverse shocks, and the rarefaction region (region with low 168  
 density) [*Yermolaev et al.*, 2009], but these types of events 169  
 are not analyzed in this paper. The method and results of 170  
 identification of several types of solar wind streams (fast, 171  
 slow, CIR and CME which includes sum of MC, ejecta, 172  
 $SHE_{MC}$  and  $SHE_{Ej}$ ) have been recently confirmed by 173  
*Thatcher and Muller* [2011]. 174

[13] In order to calculate yearly averaged values of various 175  
 parameters, we have taken into consideration that the OMNI 176  
 database contains gaps of the data from 0 to 50% of the time 177  
 of a year. This procedure has been made under the 178  
 assumption that occurrence rate of a given type of the solar 179  
 wind streams during each year is similar both in intervals of 180  
 available data and in data gaps. If during a chosen year  $i$  the 181  
 number of events of selected solar wind type  $N_i$  has been 182  
 registered in interval of existing data  $t_{di}$ , the normalized 183  
 number of the given solar wind type  $N_i^*$  in this year was 184  
 defined by multiplication of occurrence rate of the given 185  
 solar wind type  $N_i/t_{di}$  by the total duration of year  $t_{yi}$ , i.e., 186  
 $N_i^* = (N_i/t_{di}) * t_{yi}$ . The normalized number of solar wind 187  
 events is used only for studying the time variations in 188  
 occurrence rate of various types of streams (Figure 1 and 189  
 solid circles in Figure 2), while the measured number of 190  
 events is used to calculate plasma and IMF parameters 191  
 (Figure 3) and *geoeffectiveness* and efficiency of types of 192  
 events (Figures 4 and 5 and open circles and crosses in 193  
 Figure 2). When we analyzed durations of different types of 194  
 the solar wind streams, we selected intervals of the types of 195

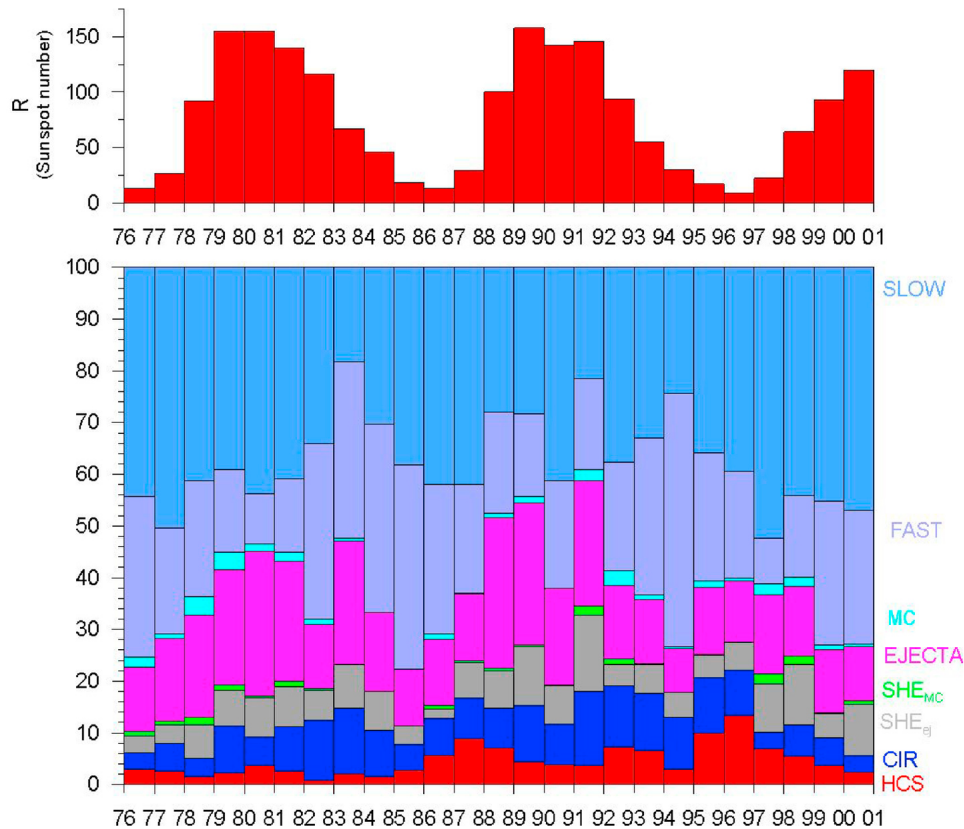


**Figure 1.** (top) Yearly average values of sunspots and (bottom) yearly average distributions of times of observations for different types of solar wind (percent).

196 streams which have not data gaps at both edges of the 197 intervals.

198 [14] Specified types of the solar wind streams were put in  
 199 correspondence to all magnetic storms for which measure-  
 200 ments of the parameters of plasma and magnetic field in the  
 201 interplanetary medium were available. This was done using  
 202 the following algorithm. If the moment of a minimum in the  
 203 *Dst* index from the list of magnetic storms falls within the  
 204 time interval of a solar wind event or is apart from it by no  
 205 more than 2 h interval, the corresponding solar wind type is  
 206 ascribed to this storm. It should be noted that, according to  
 207 the results of analysis of 64 intense (*Dst* < -85 nT) magnetic  
 208 storms in the period 1997–2002, the average time delay  
 209 between *Dst* peak and southward IMF *Bz* component is  
 210 equal to ~2 h [Gonzalez and Echer, 2005]. Similar results  
 211 were obtained in papers by Yermolaev *et al.* [2007a, 2007c].  
 212 Thus, 2 h correspond to the average time delay between the  
 213 *Dst* peak of an intense magnetic storm and the associated  
 214 peak in the southward IMF *Bz* component. Analysis of the  
 215 data showed that less 5% of points of the storm main phase  
 216 were measured during such 2 h interval between the last  
 217 point of solar wind stream and *Dst* peak.

218 [15] In order to investigate the dynamic relation between  
 219 development of parameters in interplanetary sources and in  
 220 the magnetospheric indices we apply the method of double  
 221 superposed epoch analysis (DSEA) [Yermolaev *et al.*,  
 222 2010c, 2010d]. Two reference times are used in this  
 223 method: we put together the time of storm onset (time “0”)  
 224 and time of *Dst* index minimum (time “6”), the data between

225 them we compress or expand in such a way that durations of  
 226 the main phases of all magnetic storms are equal to each  
 227 other. This DSEA method allows us to simultaneously study  
 228 interplanetary conditions resulting in the beginning and end  
 229 of magnetic storms as well as dynamics (temporal varia-  
 230 tions) of parameters during the main phase for storms with  
 231 different durations.

### 3. Results

[16] Obtained results are presented in this section devoted  
 233 to (1) observational statistics of various types of solar wind  
 234 streams, (2) probability of magnetic storm generation by  
 235 these interplanetary drivers, and (3) efficiency of magnetic  
 236 storm generation by various drivers.  
 237

#### 3.1. Occurrence Rate of Different Types of Solar Wind Streams

[17] In order to estimate geoeffectiveness of different  
 240 types of solar wind streams it is necessary to have a total list  
 241 of these types of streams during a sufficiently large time  
 242 interval and with sufficiently large statistics. Measured and  
 243 normalized numbers per year, average durations, temporal  
 244 parts in total times of observations, as well as average values  
 245 and their standard deviations of several plasma and magnetic  
 246 field parameters for various solar wind types have been  
 247 presented in our publications [Yermolaev *et al.*, 2009, 2010a,  
 248 2010b, 2010c, 2010d, 2011]. It should be noted that both  
 249 types of compressed regions (CIR and sheath), as well as  
 250

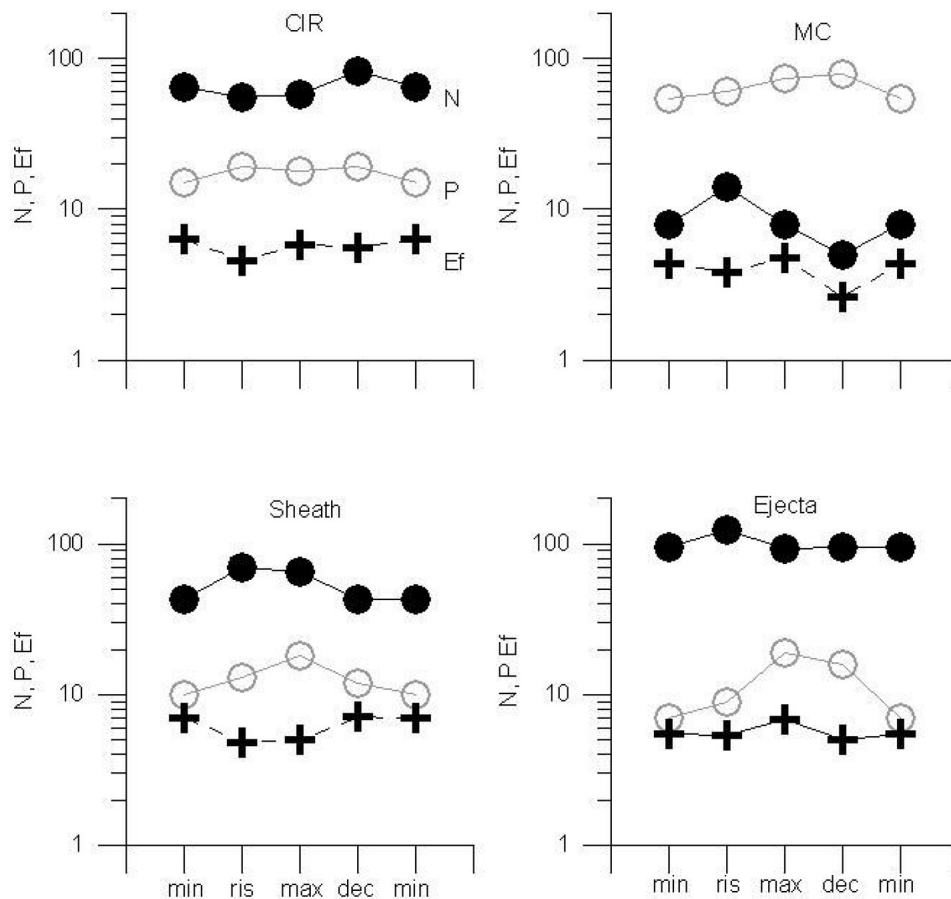


**Figure 2.** Solar cycle variations of yearly number of events (N, solid circles), probabilities (geoeffectiveness) (P, open circles), and efficiency of magnetic storm generation (Ef, crosses) for CIR, sheath, MC, and ejecta.

251 both types of sheath before MC and ejecta ( $SHE_{MC}$  and  
 252  $SHE_{Ej}$ ), have very close values of parameters, while the  
 253 parameters for 2 types of ICME (ejecta and MC) are differ-  
 254 ent. In Figure 1 (top) we present yearly average values of  
 255 sunspot numbers, and in Figure 1 (bottom) we present yearly  
 256 average distributions of times of observations for different  
 257 types of solar wind streams. Data for different types of

258 streams are shown by various color columns (see designa-  
 259 tion on the right of the figure) with height proportional to  
 260 percentage of observation time. On the average the quasi-  
 261 steady types of solar wind streams (fast, slow and HCS)  
 262 contain about 60% of all solar wind observations near the  
 263 Earth (see Table 1) but the time of disturbed types of streams  
 264 decreases down to 25% during solar minimum and increases

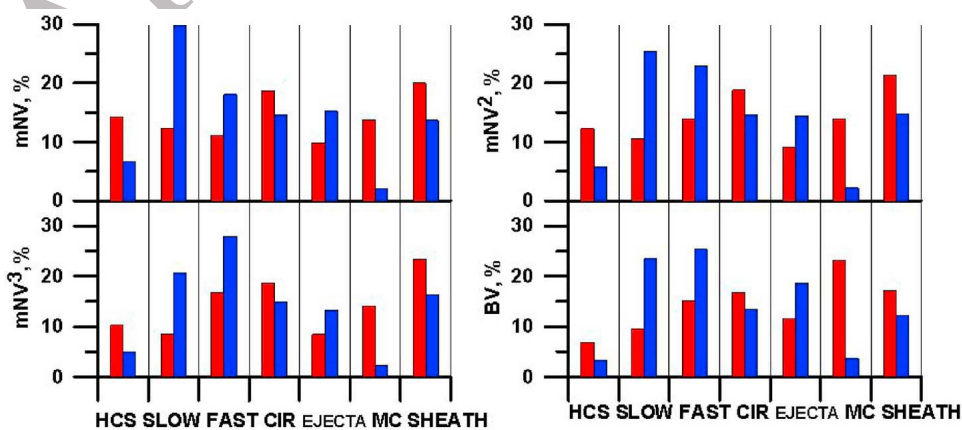


**Figure 3.** Average values (red) and integrated values (blue) mass ( $nmV$ ), momentum ( $nmV^2$ ), energy ( $nmV^3$ ), and magnetic ( $BV$ ) fluxes for different types of solar wind streams.

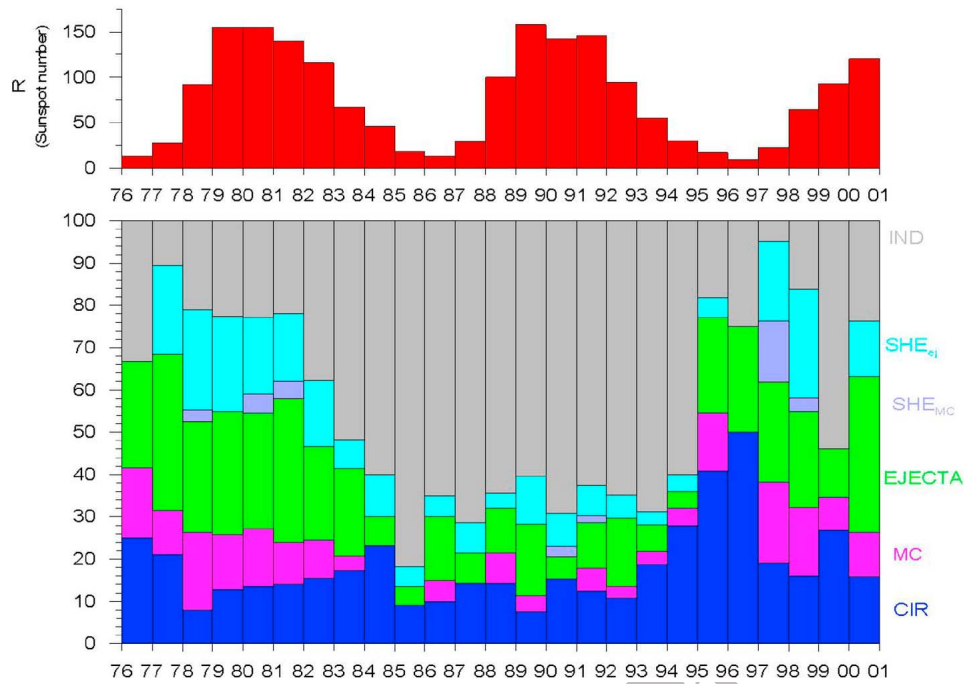


**Figure 4.** (top) Sunspot number and (bottom) year-averaged distributions of magnetic storms with  $Dst < -50$  nT over types of their interplanetary drivers (percent).

265 up to 50% during solar maximum. To increase statistics in 266 comparison with yearly averaging we made selection of data 267 over four phases of the solar cycle: minimum, rising, maxi- 268 mum and declining phases. For the same purpose we

combined two types  $SHE_{MC}$  and  $SHE_{Ej}$  and considered the 269 common type sheath. Solid circles in Figure 2 show annual 270 numbers of disturbed types of the solar wind (CIR, sheath, 271 MC and ejecta) during four phases of the solar cycle. CIR 272

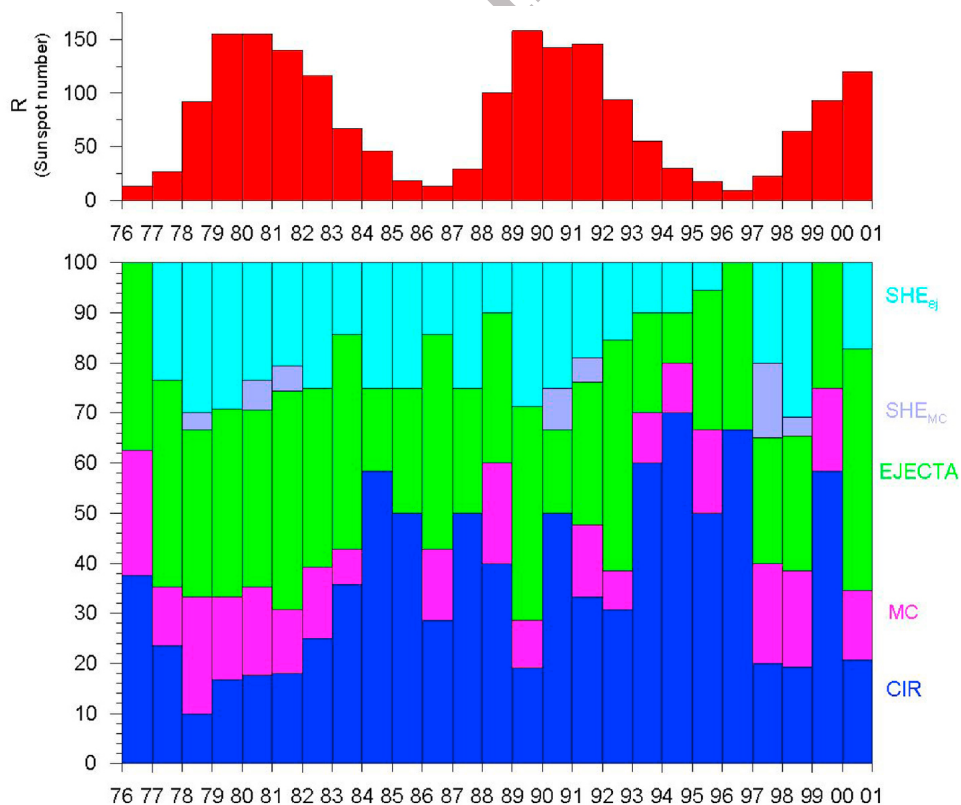


**Figure 5.** The same as in Figure 4 when IND storms were excluded from analyses.

t1.1 **Table 1.** Time Observation of Different Types of Solar Wind  
t1.2 Streams During 1976–2000

t1.4	Types of Solar Wind	Time Observations (%)
t1.5	Slow	31 ± 7
t1.6	Fast	21 ± 8
t1.7	HCS	6 ± 4
t1.8	CIR	10 ± 3
t1.9	Ejecta	20 ± 6
t1.10	MC	2 ± 1
t1.11	Sheath before ejecta	8 ± 4
t1.12	Sheath before MC	0.8 ± 0.7

273 has maximal number of events during declining phase,  
274 sheath during rising phase and maximum, and ICME (MC  
275 and ejecta) during rising phase of the cycle.

276 [18] Various types of the solar wind streams transport  
277 different values of mass, momentum, energy and magnetic  
278 field from the Sun to the Earth. To estimate contribution of  
279 all types of streams to this process we calculate two sorts of  
280 parameters for each stream type: average parameters and  
281 parameters integrated over time of observation of  
282 corresponding stream type  $\int adt$ . Figure 3 shows distribu-  
283 tions (percentage) of average values (red columns) and  
284 integrated values (blue columns) of mass ( $nmV$ ), momentum  
285 ( $nmV^2$ ), energy ( $nmV^3$ ), and magnetic ( $BV$ ) fluxes for dif-  
286 ferent types of the solar wind streams. High average values  
287 for mass, momentum, and energy fluxes are observed in  
288 compressed regions CIR and sheath and magnetic flux in  
289 MC, but their integrated values are higher in steady types of  
290 streams (fast and slow) than in disturbed types of streams. In  
291 the following sections of the paper we will analyze how the  
292 occurrence rate of different types of streams and mass,  
293 momentum, energy and magnetic field transferred by these  
294 streams influence generation of magnetic storms.

### 295 3.2. Geoeffectiveness of Interplanetary Drivers

296 [19] For the entire period of time 1976–2000, 798 mod-  
297 erate and strong magnetic storms with the intensity  $Dst \leq$   
298  $-50$  nT were observed on the Earth (see Figure 4). But only  
299 for 464 magnetic storms (i.e., for 58% of all magnetic  
300 storms) corresponding events were found in the solar wind.  
301 The sources of other 334 magnetic storms (i.e., of 42% of  
302 798 storms, grey columns in Figure 4) are indeterminate  
303 (IND type of streams), and this fact is mainly connected with  
304 the lack of data on plasma and interplanetary magnetic field  
305 which makes impossible to identify the solar wind type for

magnetic storm intervals. Figure 5 presents the distribution 306  
of storms for the case when we excluded IND storms from 307  
analysis. 308

[20] Analysis of data in Figures 1 and 5 allows us to 309  
compare the number of each type of solar wind streams with 310  
the number of magnetic storms induced by these types of 311  
streams and to calculate a probability (geoeffectiveness) of 312  
generation of magnetic storms by each types of these inter- 313  
planetary drivers (see Table 2). The values of geoeffective- 314  
ness for MC and MC with sheath ( $MC + SHE_{MC}$ ) are high 315  
and close to each other, while this value for ejecta with 316  
sheath (ejecta +  $SHE_{Ej}$ ) is significantly higher than for ejecta 317  
without sheath. The values of geoeffectiveness for sheath 318  
before MC ( $SHE_{MC}$ ) and before ejecta ( $SHE_{Ej}$ ) are close to 319  
each other, but lower than for CIR. 320

[21] Small statistics of the annual numbers of solar wind 321  
streams in Figures 1 and 5 does not allow us to clearly see 322  
solar cycle variations in geoeffectiveness of various drivers. 323  
Nevertheless larger statistics for solar cycle phases in 324  
Figure 2 (open circles) shows that all types of the solar wind 325  
streams have the lowest geoeffectiveness during the solar 326  
minimum. 327

### 3.3. Efficiency of Interplanetary Drivers 328

[22] One of important problems of connection between 329  
interplanetary conditions and magnetospheric processes is 330  
the dependence of magnetospheric activity on temporal 331  
evolution of solar wind plasma and IMF parameters 332  
including  $Bz$  and  $Ey$ . Using the DSEA method [Yermolaev 333  
*et al.*, 2010c], we found qualitative consistency between 334  
time evolution of cause ( $Bz$  and  $Ey$ ) and time evolution 335  
of effect ( $Dst$ ,  $Dst^*$  (pressure corrected  $Dst$ ),  $Kp$  and  $AE$  336  
indices) for the main phase time interval as dependence of 337  
indices on integral value of sources, for example, 338  
 $Dst^i$ . vs.  $Ey(\Sigma)^i = \int_0^i Ey(\tau)d\tau = \sum_0^i Ey^k$ ,  $i = 0, \dots, 6$ ;  $k = 0, \dots, i$ . 339

[23] Dependencies of  $Dst$  (or  $Dst^*$ ) on the integral of  $Bz$  340  
(or  $Ey$ ) over time are almost linear and parallel for different 341  
types of drivers. This fact can be considered as an indication 342  
that time evolution of the main phase of storms depends not 343  
only on current values of  $Bz$  and  $Ey$ , but also on their pre- 344  
history. The differences between these lines are relatively 345  
small ( $|\Delta Dst| < 20$  nT). Nevertheless we can make the fol- 346  
lowing comparisons. For various drivers we approximated 347  
data near the central parts of dependencies by linear func- 348  
tions and using these linear functions we calculated values of 349  
 $Dst$  (or  $Dst^*$ ) at fixed values of integral of  $Bz$  and integral of 350  
 $Ey$  ( $\int_0^i Bz(\tau)d\tau = -30$  h\*nT and  $\int_0^i Ey(\tau)d\tau = 12$  h\*mV/m). 351

t2.1 **Table 2.** Probability of Generation of Magnetic Storms With  $Dst \leq -50$  nT (Geoeffectiveness) for Different Types of Solar Wind  
t2.2 Streams During 1976–2000

t2.4	Types of Solar Wind	Number of Observations of Interplanetary Events	Number of Storms Induced by This Type of Event	Part From Identified Storms (%)	Geoeffectiveness
t2.5	CIR	717	145	31.2	0.202
t2.6	Sheath before MC	79	12	2.6	0.142
t2.7	Sheath before ejecta	543	84	18.1	0.155
t2.8	MC with sheath	79	50	13.4	0.633
t2.9	MC without sheath	22	12	2.6	0.545
t2.10	Ejecta with sheath	543	115	24.8	0.212
t2.11	Ejecta without sheath	585	46	9.9	0.078

**Table 3.** Ratio of Magnetospheric Indices to Integrated IMF  $B_z$  and  $E_y$  Fields<sup>a</sup>

Solar Wind									
Type	$Dst/B_z$	$Dst^*/B_z$	$Kp/B_z$	$AE/B_z$	$Dst/E_y$	$Dst^*/E_y$	$Kp/E_y$	$AE/E_y$	
CIR	2.4	2.8	0.18	22.7	5.0	6.8	0.45	56.8	
Ejecta	2.6	2.6	0.17	22.0	6.1	6.8	0.43	53.8	
MC	1.9	2.1	0.17	22.3	4.3	4.9	0.42	54.2	
Ejecta+MC	2.3	2.6	0.17	21.8	5.3	6.0	0.42	53.3	
Sheath	2.4	3.0	0.20	24.3	4.9	6.3	0.46	57.9	
IND	2.9	2.6	0.18	24.0	6.5	6.1	0.44	48.9	

<sup>a</sup>Ratio at fixed values of  $\int_0^t B_z(\tau)d\tau = -30 \text{ h}^*\text{nT}$  and  $\int_0^t E_y(\tau)d\tau = 12 \text{ h}^*\text{mV/m}$ . Dimensions of coefficients:  $[Dst/B_z, Dst^*/B_z, AE/B_z] = \text{nT}/(\text{h}^*\text{nT})$ ,  $[Kp/B_z] = 1/(\text{h}^*\text{nT})$ ,  $[Dst/E_y, Dst^*/E_y, AE/E_y] = \text{nT}/(\text{h}^*\text{mV/m})$ , and  $[Kp/E_y] = 1/(\text{h}^*\text{mV/m})$ .

The ratio of these calculated values of  $Dst$  (or  $Dst^*$ ) indices to the fixed values of integrated  $B_z$  (or  $E_y$ ) is a quantitative estimation of the process efficiency (see values  $Dst/B_z$ ,  $Dst/E_y$ ,  $Dst^*/B_z$  and  $Dst^*/E_y$  in Table 3). It should be noted that Nikolaeva et al. [2012] found integrated  $E_y$  threshold for generation of magnetic storms with  $Dst \leq -50 \text{ nT}$  and the used value of integral of  $E_y = 12 \text{ h}^*\text{mV/m}$  is located near this threshold (i.e., the used interval of integral of  $E_y$  contains data for almost all magnetic storms). The value  $\int_0^t B_z(\tau)d\tau = -30 \text{ h}^*\text{nT}$  was recalculated from threshold value for  $E_y$ . Taking into account that differences in “efficiency coefficients” for various drivers are mathematically significant when they differ more by than 10% (i.e.,  $0.25 \text{ nT}/(\text{h}^*\text{nT})$  for  $B_z$  and  $0.5 \text{ nT}/(\text{h}^*\text{mV/m})$  for  $E_y$ ), it is possible to note that (1) dependencies of  $Dst$  (or  $Dst^*$ ) on the integral of  $B_z$  (or  $E_y$ ) are higher in CIR, sheath and ejecta than in MC (i.e., efficiency of MC for the process of magnetic storm generation is the lowest one) and (2) efficiency of CIR, sheath and ejecta are closed to each other. Dependencies of  $Kp$  (and  $AE$ ) on integral of  $B_z$  (and  $E_y$ ) are nonlinear (there is the saturation effect for  $AE$  index) and nonparallel. Nevertheless we made the same procedure for them as for  $Dst$  and  $Dst^*$  indices and calculated estimations of efficiency for different drivers. Efficiency for  $Kp$  and  $AE$  indices is higher for CIR and sheath than for MC and ejecta.

[24] Figure 2 (crosses) presents the solar cycle variation in efficiency of magnetic storm generation  $E_f$  (value  $Dst/E_y$  in Table 3) for four interplanetary drivers. Variations in efficiency for CIR, sheath and ejecta are small in comparison with data deviation, and minimum of  $E_f$  for MC during the declining phase of the solar cycle may be connected with small statistics of MC observations. Nevertheless, it is possible to indicate that CIR has  $E_f$  minimum during the rising phase, sheath during the rising and maximum phases, and ejecta has  $E_f$  maximum during the maximum phase.

#### 4. Discussion and Conclusions

[25] The amount of the Sun’s energy flowing into the magnetosphere and causing magnetospheric disturbances, is defined by the following processes and relations: (1) relative occurrence rate of disturbed types of solar wind streams (interplanetary drivers of magnetic storms), (2) typical values of plasma and field parameters in these types of streams, (3) probability of magnetic storm generation (geoeffectiveness) for these drivers (i.e., probability of occurrence of the southward IMF  $B_z$  component in these

drivers), and (4) efficiency of physical process of magnetic storm generation for various drivers.

[26] On the basis of OMNI data for 1976–2000 we estimated and compared for the first time the entire set of these processes and relations for main set of interplanetary drivers of magnetic storms (CIR, MC, ejecta,  $SHE_{MC}$  and  $SHE_{E_y}$ ).

[27] The results of our identification of solar wind streams [Yermolaev et al., 2009] were partially compared with tabulated data of various events presented on the websites <http://star.mpae.gwdg.de> and <http://lempfi.gsfc.nasa.gov>, as well as with the ISTP Solar Wind Catalog on the website <http://www.spof.gsfc.nasa.gov/scripts/sw-cat/Catalog-events.html> and presented in papers by Cane and Richardson [2003], Richardson and Cane [2004], Huttunen et al. [2005], Dmitriev et al. [2005], Alves et al. [2006], Koskinen and Huttunen [2006], Echer et al. [2006], Zhang et al. [2007], Jian et al. [2008], Lepping and Wu [2010], and Thatcher and Muller [2011]. This comparison showed a good agreement in more than 90% of events. It is important to note that, unlike numerous papers where solar wind identifications were made for selection of only one or two stream types, we realized this approach with a single set of criteria to eight large-scale stream types and five types from them are analyzed in this paper as drivers of magnetic storms. The obtained statistical characteristics and distributions of the solar wind and IMF parameters in various types of the streams well agree with previously obtained results.

[28] During the full time from 1976 to 2000 the different types of the solar wind were observed: MC for  $2 \pm 1\%$ , ejecta for  $20 \pm 6\%$ , sheath before ejecta for  $8 \pm 4\%$ , sheath before MC for  $0.8 \pm 0.7\%$ , and CIR for  $10 \pm 3\%$  of the total observation time. About 53% of the entire observation time fell on the fast and slow solar wind (21.5% and 31.5% of time, respectively) (see Figure 1 and Table 1) [Yermolaev et al., 2010a, 2010b]. The numbers of sheath, MC and ejecta events have maximum during rising and maximum phases of the solar cycle, while CIR has maximum during declining phase (Figure 2). Our new results show that large values of mass, momentum and energy are transported from the Sun to the Earth by CIR and sheath, and of magnetic field by MC (see Figure 3).

[29] The probabilities that conditions in the interplanetary space allow the solar wind to input energy to in magnetosphere and generate magnetic storm with  $Dst \leq -50 \text{ nT}$  are about 55% for MC (63% for MC with sheath), about 20% for CIR, about 8% for ejecta (21% for ejecta with sheath) and 15% for sheath (see Table 2). Because of different occurrence rates of various solar wind streams it was found that 35% of storms were generated by ejecta with/without sheath, 31% by CIR and 24% by MC with/without sheath (about 20% by sheath before MC and ejecta). Taking into account dependence of numerical estimation on the used method of data analysis, the values of geoeffectiveness obtained by us for MC and ejecta (both with sheath and without sheath) are in a good agreement with previous result (see review by Yermolaev and Yermolaev [2010]). Our estimation of CIR geoeffectiveness (about 20%) is lower than that obtained early by Alves et al. [2006]. Geoeffectiveness of sheath, MC and ejecta has maximum during the maximum and declining phases of the solar cycle, CIR has minimum during the minimum phase (Figure 2).

458 [30] The numerical estimations made in this work show  
 459 that efficiency of MC for the process of magnetic storm  
 460 generation (for *Dst* and *Dst\** indices) is the lowest one, and  
 461 efficiency for *Kp* and *AE* indices is higher for CIR and  
 462 sheath than for MC and ejecta. Higher efficiency of the  
 463 process of magnetic storms generation by sheath than MC  
 464 are discussed in several papers [Huttunen and Koskinen,  
 465 2004; Huttunen et al., 2006; Yermolaev et al., 2007a,  
 466 2007b, 2007c, 2010d; Pulkkinen et al., 2007a; Turner et al.,  
 467 2009; Guo et al., 2011]. Our results confirm this conclusion.  
 468 These data give evidence in favor of the hypotheses of  
 469 considerable effect of density (and the dynamic and thermal  
 470 pressures) and its variations, and IMF variations on the  
 471 magnetospheric activity [see, e.g., Borovsky and Funsten,  
 472 2003; D'Amicis et al., 2007; Khabarova and Yermolaev,  
 473 2008; Weigel, 2010; and references therein].

474 [31] Figure 2 shows that there is no solar cycle correlation  
 475 between geoeffectiveness and efficiency for different types  
 476 of the solar wind streams. This fact gives evidence in favor  
 477 suggestion that geoeffectiveness (probability) of all types of  
 478 streams is connected with solar and interplanetary processes,  
 479 but not with magnetospheric ones.

480 [32] Thus obtained results show that despite the low  
 481 occurrence rate and low efficiency of magnetic clouds they  
 482 play an essential role in generation of magnetic storms due  
 483 to high geoeffectiveness of storm generation (i.e., high  
 484 probability to contain large and long-term southward IMF *Bz*  
 485 component). Geoeffectiveness of CIR and sheath are lower,  
 486 but they are compensated by higher occurrence rate and  
 487 efficiency.

488 [33] **Acknowledgments.** The authors are grateful for the opportunity  
 489 to use the OMNI database. The OMNI data were obtained from GSFC/  
 490 SPDF OMNIWeb (<http://omniweb.gsfc.nasa.gov>). This work was sup-  
 491 ported by the Russian Foundation for Basic Research, projects 07–02–  
 492 00042 and 10–02–00277a, and by Program 15 of the Physics Department  
 493 of the Russian Academy of Sciences (OFN RAN) and Program 22 of  
 494 Presidium of the Russian Academy of Sciences.

495 [34] Masaki Fujimoto thanks the reviewers for their assistance in  
 496 evaluating this paper.

497 **References**

498 Akasofu, S.-I. (1981), Energy coupling between the solar wind and the  
 499 magnetosphere, *Space Sci. Rev.*, *28*, 121–190, doi:10.1007/BF00218810.  
 500 Alves, M. V., E. Echer, and W. D. Gonzalez (2006), Geoeffectiveness of  
 501 corotating interaction regions as measured by *Dst* index, *J. Geophys.*  
 502 *Res.*, *111*, A07S05, doi:10.1029/2005JA011379.  
 503 Alves, M. V., E. Echer, and W. D. Gonzalez (2011), Geoeffectiveness of  
 504 solar wind interplanetary magnetic structures, *J. Atmos. Sol. Terr. Phys.*,  
 505 *73*, 1380–1384.  
 506 Borovsky, J. E., and M. H. Denton (2006), Differences between CME-  
 507 driven storms and CIR-driven storms, *J. Geophys. Res.*, *111*, A07S08,  
 508 doi:10.1029/2005JA011447.  
 509 Borovsky, J. E., and H. O. Funsten (2003), Role of solar wind turbulence in  
 510 the coupling of the solar wind to the Earth's magnetosphere, *J. Geophys.*  
 511 *Res.*, *108*(A6), 1246, doi:10.1029/2002JA009601.  
 512 Burlaga, L. F. (1991), Magnetic clouds, in *Physics of the Inner Heliosphere*  
 513 *II: Particles, Waves, and Turbulence*, *Phys. Chem. Space*, vol. 20, edited  
 514 by R. Schwenn and E. Marsch, Springer, New York.  
 515 Burton, R. K., R. L. McPherron, and C. T. Russell (1975), An empirical  
 516 relationship between interplanetary conditions and *Dst*, *J. Geophys.*  
 517 *Res.*, *80*, 4204–4214.  
 518 Cane, H. V., and I. G. Richardson (2003), Interplanetary coronal mass ejections  
 519 in the near-Earth solar wind during 1996–2002, *J. Geophys. Res.*,  
 520 *108*(A4), 1156, doi:10.1029/2002JA009817.  
 521 D'Amicis, R., R. Bruno, and B. Bavassano (2007), Is geomagnetic activity  
 522 driven by solar wind turbulence?, *Geophys. Res. Lett.*, *34*, L05108,  
 523 doi:10.1029/2006GL028896.  
 524 Denton, M. H., J. E. Borovsky, R. M. Skoug, M. F. Thomsen, B. Lavraud,  
 525 M. G. Henderson, R. L. McPherron, J. C. Zhang, and M. W. Liemohn

(2006), Geomagnetic storms driven by ICME- and CIR-dominated solar  
 526 wind, *J. Geophys. Res.*, *111*, A07S07, doi:10.1029/2005JA011436.  
 527 Despirak, I. V., A. A. Lubchich, A. G. Yahnin, B. V. Kozelov, and H. K.  
 528 Biernat (2009), Development of substorm bulges during different solar  
 529 wind structures, *Ann. Geophys.*, *27*, 1951–1960.  
 530 Despirak, I. V., A. A. Lubchich, and V. Guineva (2011), Development  
 531 of substorm bulges during storms of different interplanetary origins,  
 532 *J. Atmos. Sol. Terr. Phys.*, *73*, 1460–1464.  
 533 Dmitriev, A. V., N. B. Crosby, and J.-K. Chao (2005), Interplanetary  
 534 sources of space weather disturbances in 1997 to 2000, *Space Weather*,  
 535 *3*, S03001, doi:10.1029/2004SW000104.  
 536 Dungey, J. W. (1961), Interplanetary magnetic field and the auroral zones,  
 537 *Phys. Rev. Lett.*, *6*, 47–48.  
 538 Echer, E., and W. D. Gonzalez (2004), Geoeffectiveness of interplanetary  
 539 shocks, magnetic clouds, sector boundary crossings and their  
 540 combined occurrence, *Geophys. Res. Lett.*, *31*, L09808, doi:10.1029/  
 541 2003GL019199.  
 542 Echer, E., W. D. Gonzalez, and M. V. Alves (2006), On the geomagnetic  
 543 effects of solar wind interplanetary magnetic structures, *Space Weather*,  
 544 *4*, S06001, doi:10.1029/2005SW000200.  
 545 Echer, E., W. D. Gonzalez, and B. T. Tsurutani (2011), Statistical studies  
 546 of geomagnetic storms with peak *Dst* < –50 nT from 1957 to 2008,  
 547 *J. Atmos. Sol. Terr. Phys.*, *73*, 1454–1459.  
 548 Fairfield, D. H., and L. J. Cahill Jr. (1966), The transition region magnetic  
 549 field and polar magnetic disturbances, *J. Geophys. Res.*, *71*, 155–169.  
 550 Gonzalez, W. D., and E. Echer (2005), Study on the peak *Dst* and peak neg-  
 551 ative *Bz* relationship during intense geomagnetic storms, *Geophys. Res.*  
 552 *Lett.*, *32*, L18103, doi:10.1029/2005GL023486.  
 553 Gonzalez, W. D., B. T. Tsurutani, and A. L. Clúa de Gonzalez (1999), Inter-  
 554 planetary origin of geomagnetic storms, *Space Sci. Rev.*, *88*, 529–562.  
 555 Gonzalez, W. D., E. Echer, B. T. Tsurutani, A. L. Clúa de Gonzalez, and  
 556 A. Dal Lago (2011), Interplanetary origin of intense, superintense and  
 557 extreme geomagnetic storms, *Space Sci. Rev.*, *158*, 69–89, doi:10.1007/  
 558 s11214-010-9715-2.  
 559 Guo, J., X. Feng, B. A. Emery, J. Zhang, C. Xiang, F. Shen, and W. Song  
 560 (2011), Energy transfer during intense geomagnetic storms driven by  
 561 interplanetary coronal mass ejections and their sheath regions, *J. Geophys.*  
 562 *Res.*, *116*, A05106, doi:10.1029/2011JA016490.  
 563 Huttunen, K. E. J., and H. E. J. Koskinen (2004), Importance of postshock  
 564 streams and sheath region as drivers of intense magnetospheric storms  
 565 and high-latitude activity, *Ann. Geophys.*, *22*, 1729–1738, doi:10.5194/  
 566 angeo-22-1729-2004.  
 567 Huttunen, K. E. J., R. Schwenn, V. Bothmer, and H. E. J. Koskinen (2005),  
 568 Properties and geoeffectiveness of magnetic clouds in the rising, maxi-  
 569 mum and early declining phases of solar cycle 23, *Ann. Geophys.*, *23*,  
 570 625–641.  
 571 Huttunen, K. E. J., H. E. J. Koskinen, A. Karinen, and K. Mursula  
 572 (2006), Asymmetric development of magnetospheric storms during  
 573 magnetic clouds and sheath regions, *Geophys. Res. Lett.*, *33*, L06107,  
 574 doi:10.1029/2005GL024894.  
 575 Jian, L. K., C. T. Russell, J. G. Luhmann, R. M. Skoug, and J. T. Steinberg  
 576 (2008), Stream interactions and interplanetary coronal mass ejections at  
 577 0.72 AU, *Sol. Phys.*, *249*, 85–101, doi:10.1007/s11207-008-9161-4.  
 578 Khabarova, O. V., and Y. I. Yermolaev (2008), Solar wind parameters  
 579 behavior before and after magnetic storms, *J. Atmos. Sol. Terr. Phys.*,  
 580 *70*, 384–390, doi:10.1016/j.jastp.2007.08.024.  
 581 King, J. H., and N. E. Papitashvili (2005), Solar wind spatial scales in and  
 582 comparisons of hourly Wind and ACE plasma and magnetic field data,  
 583 *J. Geophys. Res.*, *110*, A02209, doi:10.1029/2004JA010649.  
 584 Koskinen, H. E. J., and K. E. J. Huttunen (2006), Geoeffectivity of coronal  
 585 mass ejections, *Space Sci. Rev.*, *124*, 169–181, doi:10.1007/s11214-006-  
 586 9103-0.  
 587 Lepping, R. P., and C.-C. Wu (2010), Selection effects in identifying mag-  
 588 netic clouds and the importance of the closest approach parameter, *Ann.*  
 589 *Geophys.*, *28*, 1539–1552, doi:10.5194/angeo-28-1539-2010.  
 590 Longden, N., M. H. Denton, and F. Honary (2008), Particle precipitation  
 591 during ICME-driven and CIR-driven geomagnetic storms, *J. Geophys.*  
 592 *Res.*, *113*, A06205, doi:10.1029/2007JA012752.  
 593 Lopez, R. E. (1987), Solar cycle invariance in solar wind proton tempera-  
 594 ture relationships, *J. Geophys. Res.*, *92*, 11,189–11,194.  
 595 Mustajab, F., and Badruddin (2011), Geoeffectiveness of the interplanetary  
 596 manifestations of coronal mass ejections and solar-wind stream–stream  
 597 interactions, *Astrophys. Space Sci.*, *331*, 91–104, doi:10.1007/s10509-  
 598 010-0428-5.  
 599 Nikolaeva, N. S., Y. I. Yermolaev, and I. G. Lodkina (2011), Dependence  
 600 of geomagnetic activity during magnetic storms on the solar wind param-  
 601 eters for different types of streams [in Russian], *Geomagn. Aeron.*,  
 602 *51*, 51–67. [*Geomagn. Aeron.*, Engl. Transl., *51*, 49–65.]  
 603



604 Nikolaeva, N. S., Y. I. Yermolaev, and I. G. Lodkina (2012), Dependence  
 605 of geomagnetic activity during magnetic storms on the solar wind param-  
 606 eters for different types of streams: 2. Main phase of storm, *Geomagn.  
 607 Aeron.*, 52, 31–40. [*Geomagn. Aeron.*, Engl. Transl., 52, 28–36.]  
 608 Plotnikov, I. Y., and E. S. Barkova (2007), Nonlinear dependence of *Dst*  
 609 and *AE* indices on the electric field of magnetic clouds, *Adv. Space  
 610 Res.*, 40, 1858–1862.  
 611 Pulkkinen, T. I., N. Partamies, K. E. J. Huttunen, G. D. Reeves, and H. E. J.  
 612 Koskinen (2007a), Differences in geomagnetic storms driven by mag-  
 613 netic clouds and ICME sheath regions, *Geophys. Res. Lett.*, 34,  
 614 L02105, doi:10.1029/2006GL027775.  
 615 Pulkkinen, T. I., N. Partamies, R. L. McPherron, M. Henderson, G. D.  
 616 Reeves, M. F. Thomsen, and H. J. Singer (2007b), Comparative statistical  
 617 analysis of storm time activations and sawtooth events, *J. Geophys. Res.*,  
 618 112, A01205, doi:10.1029/2006JA012024.  
 619 Richardson, I. G., and H. V. Cane (2004), The fraction of interplanetary  
 620 coronal mass ejections that are magnetic clouds: Evidence for a solar  
 621 cycle variation, *Geophys. Res. Lett.*, 31, L18804, doi:10.1029/  
 622 2004GL020958.  
 623 Rostoker, G., and C.-G. Falthammar (1967), Relationship between changes  
 624 in the interplanetary magnetic field and variations in the magnetic field at  
 625 the Earth's surface, *J. Geophys. Res.*, 72, 5853–5863.  
 626 Russell, C. T., R. L. McPherron, and R. K. Burton (1974), On the cause of  
 627 magnetic storms, *J. Geophys. Res.*, 79, 1105–1109.  
 628 Thatcher, L. J., and H.-R. Muller (2011), Statistical investigation of hourly  
 629 OMNI solar wind data, *J. Geophys. Res.*, 116, A12107, doi:10.1029/  
 630 2011JA017027.  
 631 Tsurutani, B. T., and W. D. Gonzalez (1997), The interplanetary causes of  
 632 magnetic storms: A review, in *Magnetic Storms*, *Geophys. Monogr. Ser.*,  
 633 vol. 98, edited by B. T. Tsurutani et al., pp. 77–89, AGU, Washington,  
 634 D. C.  
 635 Tsurutani, B. T., W. D. Gonzalez, F. Tang, S. I. Akasofu, and E. J. Smith  
 636 (1988), Origin of interplanetary southward magnetic fields responsible  
 637 for major magnetic storms near solar maximum (1978–1979), *J. Geophys.  
 638 Res.*, 93(A8), 8519–8531.  
 639 Turner, N. E., W. D. Cramer, S. K. Earles, and B. A. Emery (2009), Geof-  
 640 ficiency and energy partitioning in CIR-driven and CME-driven storms,  
 641 *J. Atmos. Sol. Terr. Phys.*, 71, 1023–1031.  
 642 Weigel, R. S. (2010), Solar wind density influence on geomagnetic storm  
 643 intensity, *J. Geophys. Res.*, 115, A09201, doi:10.1029/2009JA015062.  
 644 Xu, D., T. Chen, X. X. Zhang, and Z. Liu (2009), Statistical relationship  
 645 between solar wind conditions and geomagnetic storms in 1998–2008,  
 646 *Planet. Space Sci.*, 57, 1500–1513.  
 Yermolaev, Y. I., and M. Y. Yermolaev (2002), Statistical relationships  
 between solar, interplanetary, and geomagnetospheric disturbances,  
 1976–2000, *Cosmic Res., Engl. Transl.*, 40(1), 1–14.  
 Yermolaev, Y. I., and M. Y. Yermolaev (2006), Statistic study on the geo-  
 magnetic storm effectiveness of solar and interplanetary events, *Adv.  
 Space Res.*, 37(6), 1175–1181.  
 Yermolaev, Y. I., and M. Y. Yermolaev (2010), Solar and interplanetary  
 sources of geomagnetic storms: Space weather aspects, *Izv. Russ. Acad.  
 Sci. Atmos. Oceanic Phys., Engl. Transl.*, 46(7), 799–819.  
 Yermolaev, Y. I., M. Y. Yermolaev, I. G. Lodkina, and N. S. Nikolaeva  
 (2007a), Statistic investigation of heliospheric conditions resulting in  
 magnetic storms, *Cosmic Res., Engl. Transl.*, 45(1), 1–8.  
 Yermolaev, Y. I., M. Y. Yermolaev, I. G. Lodkina, and N. S. Nikolaeva  
 (2007b), Statistic investigation of heliospheric conditions resulting in  
 magnetic storms: 2, *Cosmic Res., Engl. Transl.*, 45(6), 461–470.  
 Yermolaev, Y. I., M. Y. Yermolaev, N. S. Nikolaeva, and L. G. Lodkina  
 (2007c), Interplanetary conditions for CIR-induced and MC-induced geo-  
 magnetic storms, *Bulg. J. Phys.*, 34, 128–135.  
 Yermolaev, Y. I., N. S. Nikolaeva, I. G. Lodkina, and M. Y. Yermolaev  
 (2009), Catalog of large-scale solar wind phenomena during 1976–  
 2000, *Kosm. Issled.*, 47(2), 99–113. [*Cosmic Res.*, Engl. Transl., 47(2),  
 81–94.]  
 Yermolaev, Y. I., N. S. Nikolaeva, I. G. Lodkina, and M. Y. Yermolaev  
 (2010a), Relative occurrence rate and geoeffectiveness of large-scale  
 types of the solar wind, *Kosm. Issled.*, 48(1), 3–32. [*Cosmic Res.*, Engl.  
 Transl., 48(1), 1–30.]  
 Yermolaev, Y. I., N. S. Nikolaeva, I. G. Lodkina, and M. Y. Yermolaev  
 (2010b), Large-scale solar wind structures: Occurrence rate and geoeffec-  
 tiveness, *AIP Conf. Proc.*, 1216, 648–651.  
 Yermolaev, Y. I., N. S. Nikolaeva, I. G. Lodkina, and M. Y. Yermolaev  
 (2010c), Specific interplanetary conditions for CIR-, sheath-, and  
 ICME-induced geomagnetic storms obtained by double superposed  
 epoch analysis, *Ann. Geophys.*, 28, 2177–2186.  
 Yermolaev, Y. I., I. G. Lodkina, N. S. Nikolaeva, and M. Y. Yermolaev  
 (2010d), Statistical study of interplanetary condition effect on geomag-  
 netic storms, *Kosm. Issled.*, 48(6), 499–515. [*Cosmic Res.*, Engl. Transl.,  
 48(6), 485–500.]  
 Yermolaev, Y. I., I. G. Lodkina, N. S. Nikolaeva, and M. Y. Yermolaev  
 (2011), Statistical study of interplanetary condition effect on geomagnetic  
 storms: 2. Variations of parameters, *Cosmic Res., Engl. Transl.*, 49(1),  
 21–34.  
 Zhang, J., et al. (2007), Solar and interplanetary sources of major geomag-  
 netic storms (*Dst* < –100 nT) during 1996–2005, *J. Geophys. Res.*, 112,  
 A10102, doi:10.1029/2007JA012321.

Article